

# Localizations on Complex Networks

Guimei Zhu<sup>1,2</sup>, Huijie Yang<sup>2,3</sup>, Chuanyang Yin<sup>1,2</sup>, and Baowen Li<sup>2,4\*</sup>

<sup>1</sup> *Department of Modern Physics, University of Science and Technology of China, Hefei Anhui 230026, China*

<sup>2</sup> *Department of Physics and Centre for Computational Science and Engineering, National University of Singapore, Singapore 117542*

<sup>3</sup> *School of Management, Shanghai University for Science and Technology, Shanghai 200092, China*

<sup>4</sup> *NUS Graduate School for Integrative Sciences and Engineering, Singapore 117597, Republic of Singapore*

(Dated: February 18, 2022)

We study the structure characteristics of complex networks from the representative eigenvectors of the adjacent matrix. The probability distribution function of the components of the representative eigenvectors are proposed to describe the localizations on networks where the Euclidean distance is invalid. Several quantities are used to describe the localization properties of the representative states, as the participation ratio, the structural entropy, the probability distribution function of the nearest neighbor level spacings for spectra of complex networks. The whole cellular networks in real world, the Watts-Strogatz small world and Barabasi-Albert scale-free networks are considered. The networks have nontrivial localization properties due to the nontrivial topological structures. It is found that the ascend-ranked series of the occurring probabilities at the nodes behave generally multi-fractal. This characteristic can be used as a structure measure of complex networks.

PACS numbers: 89.75.Hc, 72.15.Rn, 05.50.+q, 05.45.Df

## I. INTRODUCTION

Recent years have witness an avalanche of research on complex network and its applications in diverse fields [1]. Structure measures of complex networks are the cornerstone to understand relations between the structures, dynamics and functions. Real world networks generally have nontrivial properties as the small-world [2], scale-free [3], motif [4], modularity, hierarchy [5], fractal [6] and so on. The small-world effect is that in average the nodes can reach each other with only a small number of hops. The scale-free refers to the number of edges per node obeys a right-skewed distribution. It is also found that some special subgraphs containing several connected nodes, called motifs, occur with significant probabilities compared with that in the corresponding randomized networks. These three individual, pair or local pattern-based properties are called micro-properties. On the other hand, the modularity is a kind of macro-property represents that a network can be separated into loosely connected groups within which the nodes are densely connected, respectively.

To a certain degree, dynamics on networks can be regarded as the transport processes of mass, energy, signal and/or information at different structure scales [7, 8]. Sometimes we have to deal with networks with unreasonable large number of nodes and edges, e.g., the neuron networks and the World-Wide-Web networks, when designing a coarse-grain procedure is essential [9]. The patterns at different scales may provide a reasonable solution to these problems. It is found that some real world networks have hierarchical structures, in which the small-

world and the scale-free properties can coexist [5]. Moreover, many real world networks behave self-similar at different structure levels (fractal) [6].

Though great progresses have been archived, the measures of complex networks are not yet fully understood. Just as pointed out by Newman [10], that our techniques for analyzing networks are at present time no more than a grab-bag of miscellaneous and largely unrelated tools, and we still do not have a systematic program for characterizing network structures. Furthermore, the measures of network structures, such as the micro-properties, the patterns at different scales and the macro-properties, are generally a simple application of the concepts in graph theory, bioinformatics, social science and fractal theory, namely, they are not dynamics-based. We can not expect simple and reasonable relations between the measures and the dynamical processes on networks.

The lack of powerful tools to characterize network structures is an essential bottleneck to understand dynamical processes on networks. One typical example is the synchronizabilities of complex networks. Detailed works show that almost all the structure measures affect the synchronizabilities in complicated ways [11], based upon which we can not reach a clear picture of the mechanisms for synchronization processes on networks.

Dynamics-based measures of complex networks may be the key to the problems. The structures of complex networks can induce nontrivial properties to the physical processes occurring on them. The physical processes in turn can be used as the probe to capture the structure properties. Well studied dynamical processes, such as the random walks [12, 13] and the Boolean dynamics [14], can be good candidates as probes. To cite an example, the random walks on complex networks that biased towards a target node show a localization-delocalization transition [12].

---

\*Electronic address: phylibw@nus.edu.sg

In the present paper, we map networks to large clusters, namely, the nodes and edges to atoms and bonds between them, respectively. The localization properties of electrons in the clusters can be used as measures of the structure properties of the networks. We try to detect the global symmetries from the spectra and the eigenvectors of complex networks. Very recently, much attentions have been focused on detecting global characteristics embedded in spectra of complex networks due to their potential application in understanding the organization mechanisms and the synchronization dynamics of complex networks [8, 15, 16]. To our best knowledge, it is the first time to detect the global characteristics of complex networks from the eigenvectors which contain more information about the system than eigenvalues.

Besides as a measure of network structures, the structure-induced localization may have potential application in understanding the electronic properties of materials such as conductive polymers and carbon nanonets. The intrachain windings in conductive polymers can introduce long-range edges into the original one dimensional (1-D) systems, resulting in nontrivial network structures [17, 18]. It is also found that random networks of carbon nanotubes, called nanonets, can mimic a variety of basic electronic functions from the conductive properties of metals to the less conductive characteristics of semiconductors [19]. Indeed, nanonets have paved the way for the carbon to serve as the foundation for future electronic devices. The effect of network structures on electronic properties is one of the most active topics in recent years [7, 20].

The paper is organized as follows: In Sec.II the concept of localization on complex networks is presented. The occurring probabilities on the nodes are proposed to describe quantitatively the localization effects. In Sec. III the methods to measure the localization properties are described in detail. The participation ratio, the structural entropy and the probability distribution function of the nearest neighbor level spacings of spectra are used to illustrate the localization in a global way. The wavelet transform is then used to find the detailed structure properties of the probability distribution function of the occurring probabilities on the nodes. As examples, we consider the Watts Strogatz small-world and the Barabasi-Albert scale-free modeling networks and the whole cellular networks in real world. The results are shown in Sec. IV. We will be shown that the global symmetries in networks can induce multi-fractal structures in the eigenvectors. As a conclusion, the nontrivial structures of complex networks can induce significant localizations, which in turn can be used as a global measure of the structure symmetries.

## II. THE LOCALIZATIONS ON NETWORKS

We consider a undirected complex network with  $N$  identical nodes, whose topological structure can be de-

scribed by an adjacent matrix  $A$ . The elements  $A_{ij}$  are 1/0 if the nodes  $i$  and  $j$  are connected/disconnected, respectively. If we consider the nodes as atoms and the edges as bonds, the network can be mapped to a large molecule [16]. For an electron moving in such a molecule, the tight-binding Hamiltonian is,

$$\mathcal{H} = \sum_{n=1}^N \varepsilon_n \cdot |n\rangle \langle n| + \sum_{m \neq n}^N A_{mn} \cdot t_{mn} \cdot |m\rangle \langle n|, \quad (1)$$

where  $\varepsilon_n$  is the site energy and  $t_{mn} \cdot A_{mn}$  the hoping integral for the bond between sites  $m$  and  $n$ .

A tight-binding Hamiltonian of Eq.(1) is usually used to study the disorder-induced localizations. In the present form, the matrix  $A$  is explicitly introduced to describe the structure of the system. For a one dimensional (1-D) perfect regular lattice, we have  $\varepsilon_n = \varepsilon, t_{mn} = t$  and  $A_{mn} = \delta(m - n \pm 1)$ . The Bloch wave function of an electron extends all over this perfect regular lattice. Disorder structures can induce a transition from extended to localized states. The wave function for a localized state decreases exponentially with the distance from its center. The disorder effects include the random distributions of the site energies ( $\varepsilon_n$ ), the hoping integrals ( $t_{mn}$ ) and the edges in structures ( $A_{mn}$ ). The disorders come from the different kinds of atoms on the lattice points, the differences of the separations of successive lattice points and the randomness in structures. At the same time, there may be some symmetries in the distributions of the site energies, the hoping integrals and the edges, which may lead to delocalization of the wave functions.

In the usual Anderson model [21], the disorder effect due to the random distribution of the site energies is considered, i.e.,  $\varepsilon_n$  is a random variable satisfying a certain distribution probability function while  $t_{mn} = t, A_{mn} = \delta(m - n \pm 1)$ . The site energies may obey a special distribution rather than that in the Anderson model, as a periodic [22] or a power-law [23] function. In literatures [24, 25], a one-dimensional quasicrystal model is introduced that the separation of two successive lattice points takes one of the two values  $u$  and  $v$ . This model considers the disorder effect of the distribution of the hoping integrals. We have  $\varepsilon_n = \text{const.}, t_{mn} = t_u$  or  $t_v$  and  $A_{mn} = \delta(m - n \pm 1)$ .  $t_u$  and  $t_v$  are the hoping integrals corresponding to the separations  $u$  and  $v$ , respectively. It is found that quantum systems with quasi-periodic structures will be in an intermediate state, which can be described with critical wave functions. A critical wave function obeys a power-law with respect to the distance from its center.

To investigate the problems as vibration spectra of glasses, instantaneous normal modes in liquids, electron hopping in amorphous semiconductors and combinatorial optimization, Euclidean random matrix (ERM) models are widely used in literatures [26], in which the disorder is due to the random positions of the sites, and the matrix elements are given by a deterministic function of the distances.

The models mentioned above generally focus on the disorder effects of the site energies and the hopping integrals. These models have also been extended to nontrivial structured systems such as the Cayley tree [27] and the small-world networks [17]. Nontrivial effects of the structures of the systems are reported, but the interplay between the disorders due to the site energies and that due to the structures makes it difficult to distinguish the structure disorder effect from the site energy disorder effect.

In the networks considered in the current paper, however, the nodes are all identical and the disorder effect comes from the nontrivial topological structure. We focus our attentions on the disorder effect of the network structure, that is, we assign  $\varepsilon_n = 0$  and  $t_{mn} = 1$ , which leads  $H = A$ . The localization on the network refers to the network structure-induced characteristics of the wave functions for this system. The usual Anderson model [21] is a special case that in the networks there exist connections only between the nearest neighbors in Euclidean space.

Statistically, the structures of networks should display certain symmetries due to the general rules obeyed in the construction of the networks. Recent works demonstrate that many theoretical and real world networks have statistically self-similar structures [6]. Therefore, there are two competitive mechanisms determining the wave function property, the randomness of the bonds in the networks tends to cause localization of wavefunction, whereas the symmetries of the networks intend to make wave function extended. We thus expect rich structures embedded in the wave functions. As it is well known, aperiodic crystals lead to the fractal wave functions [25, 28]. An interesting question is then, how the global symmetries of networks affect the localization properties. The localization can be used as a probe of the characteristics of the network structures.

The states in the center of the energy band have the best chance to remain as extended for a moderately disordered system. The eigenvector corresponding to the special eigenvalue close to the center of the spectrum for a network, denoted by  $E_c$ , is employed as the representative state to illustrate the characteristics of the considered system.

In the traditional study of wave function localization, the physical systems have deterministic structures in real world Euclidean space, which leads to natural definitions of the localized, intermediate and extended states of the systems. Obviously, these definitions are invalid for general complex networks without deterministic structures in Euclidean space. In this paper, we describe the localization effects with the probability distribution function (PDF) of the occurring probabilities at the nodes, i.e., the values of the components for the representative eigenvector. Based on the PDF of the occurring probabilities, the traditional definitions are extended to a much more general version to describe the localization properties on complex networks.

In Euclidean space, for a state  $\Psi(r)$ , the occurring probability is  $\rho(r) = |\Psi(r)|^2 \equiv F(r)$ . Because the value of the distance  $r$  distributes homogeneously in the considered region, we can regard it as a homogeneously distributed random variable. The direct sampling method in Monte Carlo simulations tells us that the probability distribution of  $\rho$  should be  $P(\rho) \propto \frac{dF^{-1}(\rho)}{d\rho}$ . Hence, it is reasonable to define the localized, critical and perfectly extended states on complex networks with the PDFs of the occurring probabilities,

$$P(\rho) \propto \begin{cases} \delta(\rho - \rho_0), & \text{extended} \\ \rho^{-(1+\eta)} | \eta > 0, & \text{critical} \\ \rho^{-(1+\eta)} | \eta = 0, & \text{localized} \end{cases} . \quad (2)$$

The PDF of the representative function is a very powerful measure to capture the localization properties. It can be used to find the localization properties without using distance in real world Euclidean space.

Because no derivative exists for a fractal wave-function in Euclidean space, the extension procedure in defining critical and localized states on networks can not be simply used to define fractal property on networks with the PDF of the occurring probabilities. In the present paper, we detect directly the fractal characteristics in the ascend-ranked series of the the occurring probabilities, as described in detail in Section III(C).

### III. METHODS

#### A. Structural Entropy

We denote the representative state with  $V = (V_1, V_2, \dots, V_N)$ . The occurring probabilities at the nodes are  $\rho_m = |V_m|^2$ ,  $m = 1, 2, \dots, N$ . The localization extent of the state can be described quantitatively with the participation ratio [29, 30],

$$Q = \frac{1}{N \cdot \sum_{m=1}^N \rho_m^2} . \quad (3)$$

For a perfect extended state we have  $Q = 1$ , while for a state strongly localized on one node it tends to  $\frac{1}{N}$ . Generally,  $Q$  should be in the range of  $[\frac{1}{N}, 1]$ .

However, this participation ratio can capture only the primary-level complexity in the localization properties, namely, the extension of the representative eigenvector to  $N \cdot Q$  nodes on the network. Many PDFs with different localization behaviors may result in the same  $Q$ . The simplest one is a step-like function that on  $N \cdot Q$  nodes the occurring probabilities are  $\frac{1}{N \cdot Q}$ , while on the left  $N \cdot (1 - Q)$  nodes the occurring probabilities are 0.

The secondary-level complexity in the localization properties is the deviation of the PDF from the step-like function. This deviation corresponds to the shape of

the PDF, which can be extracted by using the structural entropy [31],

$$S_{str} = - \sum_{m=1}^N \rho_m \ln \rho_m - \ln(Q \cdot N). \quad (4)$$

For the simple step-like condition, we have  $S_{str} = 0$ .  $S_{str} \neq 0$  tells us the shape deviation of PDF from the simple one.

The pair of localization quantities,  $(Q, S_{str})$ , is widely used up to date to describe the localization in disordered and aperiodic systems, and the statistical analysis of spectra in diverse fields such as quantum chemistry, condensed matter physics, and quantum chaos [32, 33].

### B. Statistical Properties of the Spectra

The localization property can also be described with the random matrix theory (RMT) [30, 34, 35]. RMT is initially developed to understand the energy levels of complex nuclei and other kinds of complex quantum systems. Recently, the RMT theory has been proposed to capture the structure and dynamical properties of complex networks [15].

One of the most important quantities in the theory is the PDF for the nearest neighbor level spacings (NNLS) of the spectrum. It is theoretically and numerically confirmed that at the localization and the extended states the PDFs of the NNLS should be Poisson and Wigner-Dyson distribution, respectively [37–39]. Generally, for an intermediate state, the PDF obeys the Brody distribution,

$$U(s) = \frac{\beta}{\xi} s^{\beta-1} \exp \left[ - \left( \frac{s}{\xi} \right)^\beta \right], \quad (5)$$

where  $s$  is the NNLS and  $\xi$  the characteristic distribution width. The Poisson and the Wigner-Dyson distributions are the two extremes with  $\beta = 1$  and  $\beta = 2$ , respectively.

Introducing the accumulated function,  $C(s) = \int_0^s U(x) dx$ , some trivial calculations lead to,

$$\ln R(s) \equiv \ln \left[ \ln \left( \frac{1}{1 - C(s)} \right) \right] = \beta \ln s - \beta \ln \xi. \quad (6)$$

From this formula we can testify the Brody distribution and determine reliably the values of the parameters  $\beta$  and  $\xi$ .

To make the spacings  $s$  in units of local mean level spacing, we should conduct a standard procedure, called unfolding. Denoting the spectrum of a network with  $\lambda_1, \lambda_2, \dots, \lambda_N$ , the accumulation density function for the spectrum is  $G(\lambda_m) = m, m = 1, 2, \dots, N$ . Fitting this relation with a polynomial function, we can separate it into a smooth part and a fluctuation part as,

$$G(\lambda_m) = G_{av}(\lambda_m) + G_f(\lambda_m). \quad (7)$$

The NNLS can be obtained as,  $s_i = G_{av}(\lambda_{i+1}) - G_{av}(\lambda_i), i = 1, 2, \dots, N - 1$ . For a complex network, we generally have not enough knowledge on its spectrum, when the polynomial function fitting method can lead to a reliable result. In this paper, the order of the polynomial function is 17.

### C. Wavelet Transform

The detailed properties for the PDF of the occurring probabilities can be used as the measure of the global structure symmetries. However, determining this PDF is a nontrivial task [40]. Assume the probability values have been sorted in ascending order, namely,  $\rho = \{\rho_1 \leq \rho_2 \leq \dots \leq \rho_N\}$ , which can be regarded as the profile of the nearest spacing series,  $\Delta\rho = \{\rho_2 - \rho_1, \rho_3 - \rho_2, \dots, \rho_N - \rho_{N-1}\}$ . The local structures of  $\Delta\rho$  can tell us the probability distribution function of  $\rho$ . It is found that the series  $\rho$  generally behaves multi-fractal.

The wavelet transform (WT) [41] is used to detect the fractal properties embedded in the ascend-ranked series  $\rho$ . The increasing trend in the series  $\rho$  makes the box-counting-based techniques invalid to quantify the local scalings. In the wavelet transform, the contributions of the polynomial trends can be removed effectively. A multi-fractal series can be decomposed into many subsets characterized by different local Hurst exponent  $h$ , which quantifies the local singular behavior and thus relate to the local scaling of the series. The statistical properties of these subsets can be quantified by the fractal dimension  $D(h)$  of the subset whose local Hurst exponent is  $h$ .

As a standard procedure, we first find the WT maximal values,  $\{T_g(a, \rho_k(a)) | k = k_1, k_2, \dots, k_J\}$ , where  $a$  is the given scale. The partition function should scales in the limit of small scales as,

$$Z(a, q) = \sum_{k=k_1}^{k_J} |T_g(a, \rho_k(a))|^q \sim a^{\tau(q)}. \quad (8)$$

The fractal dimension  $D(h)$  can be obtained through the Legendre transform,

$$D(h) = qh - \tau(q), \quad h = \frac{d\tau(q)}{dq}. \quad (9)$$

For a mono-fractal structure we have a linear relation,  $\tau(q) = qH - 1$ .  $H$  is the global Hurst exponent. For positive and negative  $q$ ,  $\tau(q)$  reflects the scaling of the large fluctuations and small fluctuations, respectively.

We use the real analytic wavelet  $g^{(n)}$  among the class of derivatives of the Gaussian function, by which the polynomial trends up to  $n$  order can be removed. The results

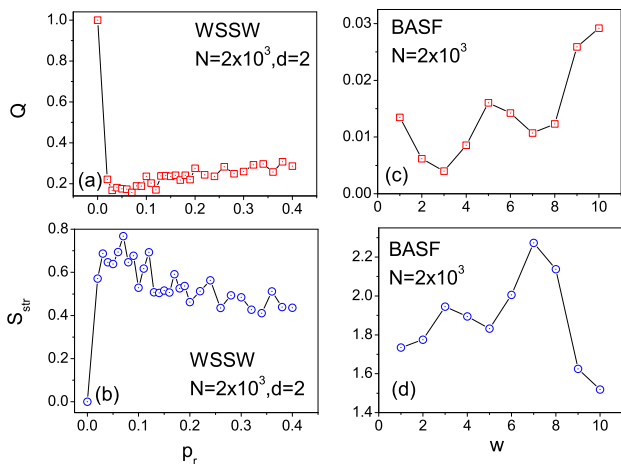


FIG. 1: (Color online) The localization quantities ( $Q, S_{str}$ ) for the WSSW and BASF networks. There exist complex relations between  $p_r$  or  $w$  and ( $Q, S_{str}$ ) for the BASF and WSSW networks. For the WSSW networks, from  $p_r = 0$  to  $p_r = 0.02$  there exists an abrupt decrease/increase in value of  $Q/S_{str}$ , as shown in (a)-(b) respectively. Then with the increase of the rewiring probability  $p_r$  the participation ratio tends to increase while the structural entropy tends to decrease; (c)-(d) Results for the BASF networks.

with  $n = 7$  are presented.  $n = 5$  and  $n = 6$  lead almost the same results. As comparison, we detect also the scaling behaviors in the randomized series  $\rho_R$ , called shuffled series.

In this paper, we are interested in the characteristic point at which the fractal dimension reaches its maximum value, ( $h_c, D(h_c)$ ). It can tell us the non-homogeneous distribution of the series  $\rho$  and the fractal characteristics of the principal subset.

#### IV. NUMERICAL RESULTS

We examine the localization behaviors for the cellular networks [42], which are compiled by using a graph-theoretical representation of all the biochemical pathways based upon the WIT integrated-pathway genome database of 43 species from Archaea, Bacteria and Eukarya [43]. The whole cellular networks consider the cellular functions as intermediate metabolism and bioenergetics, information pathways, electron transport, and transmembrane transport. The direct edges are replaced simply with non-directed edges. We consider only the cellular networks with the sizes larger than 500.

We study also the localization behaviors for the the Watts-Strogatz small-world (WSSW) [2] and the Barabasi-Albert scale-free (BASF) [3] networks. For the WSSW model, we construct firstly a regular circle lattice with each node connecting with its  $d$  right-handed nearest neighbors. For each edge we rewire it with probability  $p_r$  to another randomly selected node. Self- and double-

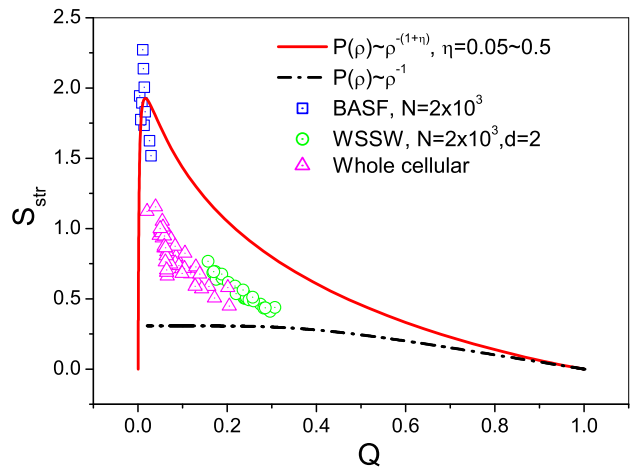


FIG. 2: (Color online) The relations of  $S_{str}$  versus  $Q$  for the WSSW, BASF and whole cellular networks. The localization quantities for the distributions,  $P(\rho) \sim \rho^{-(1+\eta)}$  and  $P(\rho) \sim \frac{1}{\rho}$ , namely, the critical and localized states, are shown as references. Starting from  $\rho(r) \sim r^{-\sigma}$ , the set of normalized values of  $\rho(\frac{n}{N}), n = 1, 2, \dots, N$  can be regarded as the critical state. Assigning  $\sigma = 1 \sim 10$ , the corresponding values of  $\eta$  are  $0.5 \sim 0.05$ .  $N$  is the size of the considered networks. The same procedure is also used to generate the localized states by starting from  $\rho(r) \sim \exp(-\mu r)$ . The localized states with  $\mu = 0.01 \sim 100$  are generated. The localization properties of the BASF networks can be captured by the critical state with extremely significantly small values of  $\eta$ . The WSSW and whole cellular networks are generally in between the two typical states.

edges are forbidden. By this way, we can introduce randomness into the resulting networks. Moreover, compared with that for the initial regular lattice, the rewiring procedure may introduce also “long-range” edges to the resulting networks, which can reduce significantly the average number of hops required for the nodes to reach each other. This is the so-called small-world effect.

The BASF networks are the results of a preferential growth mechanism, which exists widely in diverse fields. Starting from several connected nodes as a seed, at each growth step a new node is added and  $w$  edges are established between this node and the existing network. The probability for an existing node being connected with the new node is proportional to its degree. Self- and double-edges are forbidden. For the resulting networks, the number of edges per node obeys a power-law, namely, no characterized scale exists in this distribution.

Figure 1 presents the localization quantities, ( $Q, S_{str}$ ), for the networks. For the WSSW networks, the randomness introduced by the rewiring procedure has two competitive effects, the long-range edges which favors the extension, and the broken of symmetry which induces the localization. For the BASF networks, the increase of  $w$  increases the heterogeneity and the connections between the nodes, which induce the localization and the

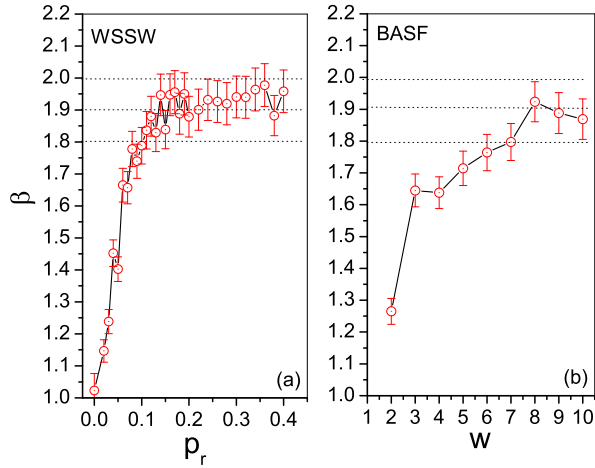


FIG. 3: (Color online) The value of Brody parameter  $\beta$  versus network parameters  $p_r$  and  $w$ . (a) WSSW networks; (b) BASF networks.

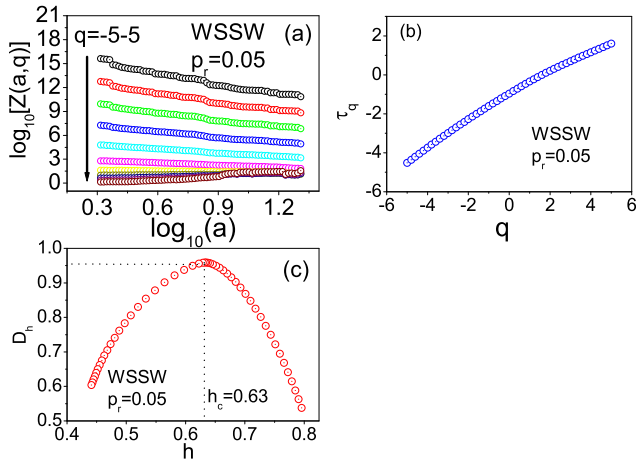


FIG. 4: (Color online) The multi-fractal scaling characteristics of the ascend-ranked series  $\rho$  for the real world, the WSSW and the BASF networks. The multi-fractal behavior for the WSSW network with  $d = 2$ ,  $N = 2000$  and  $p_r = 0.05$  is presented as a typical example. In the whole range of  $q = -5 \sim 5$ , there is only one characteristic point,  $(h_c, D(h_c)) = (0.63, 0.958)$ .

extension, respectively. Hence, there exist complex relations between  $p_r$  or  $w$  and  $(Q, S_{str})$  for the two kinds of networks, as shown in Fig.1(a)-(b) and (c)-(d), respectively. For the WSSW networks, the participation ratio decreases rapidly from 1 to 0.22 when  $p_r$  changes slightly from 0 to 0.02, and then goes up gradually with the increase of  $p_r$ . As for the structural entropy, it increases abruptly when  $p_r$  changes from 0 to 0.02, after that it decreases gradually with the increase of  $p_r$ .

Figure 2 shows  $S_{str}$  versus  $Q$ . As references, we calculate also the localization quantities for the critical and the localized states, namely,  $P(\rho) \sim \rho^{-(1+\eta)}$  and  $P(\rho) \sim \frac{1}{\rho}$ ,

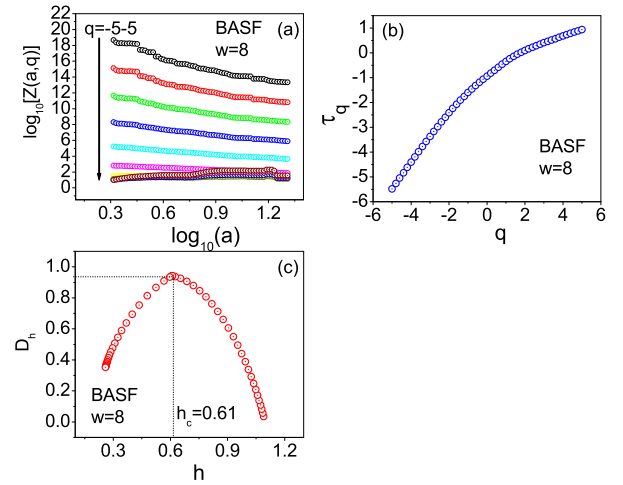


FIG. 5: (Color online) The multi-fractal scaling characteristics of the ascend-ranked series  $\rho$  for the real world, the WSSW and the BASF networks. The multi-fractal behavior for the BASF network with  $w = 8$  and  $N = 2000$  is presented as a typical example. In the whole range of  $q = -5 \sim 5$ , there is only one characteristic point,  $(h_c, D(h_c)) = (0.61, 0.942)$ .

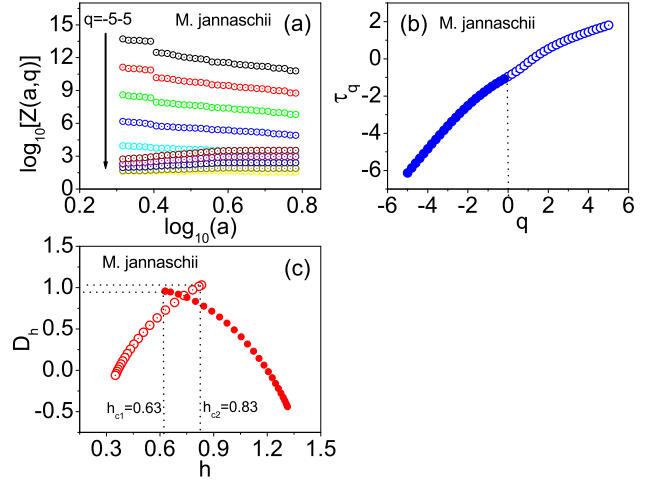


FIG. 6: (Color online) The branched multi-fractal scaling characteristics of the ascend-ranked series  $\rho$  for the real world and modeling networks. The branched multi-fractal behavior for the whole cellular network of *M. jannaschii* is presented as a typical example. The two branches  $q < 0$  and  $q > 0$  lead to different characteristic points,  $(h_{c1}, D(h_{c1})) = (0.63, 0.96)$  and  $(h_{c2}, D(h_{c2})) = (0.83, 1.03)$ .

respectively. Starting from  $\rho(r) \sim r^{-\sigma}$ , we calculate the values of  $\rho(\frac{n}{N})$ ,  $n = 1, 2, \dots, N$ . The resulting normalized values can be regarded as the localized state. The critical states with  $\sigma = 1 \sim 10$  are calculated, and the corresponding values of  $\eta$  are  $0.5 \sim 0.05$ , respectively.  $N$  is the size of the considered networks. The same procedure can be used to generate the localized states by

starting from  $\rho(r) \sim \exp(-\mu r)$ . The localized states with  $\mu = 0.01 \sim 100$  are generated.

The localization properties of the BASF networks can be captured by the critical states with extremely small values of  $\eta$ . The WSSW and whole cellular networks are generally inbetween the two typical (localized and extended) states .

We can find that the PDFs of the NNLS for all the networks can be described very well by using the Brody distribution in a unified way. The results for the parameter  $\beta$  are shown in Fig.3. For the WSSW networks, with the increase of the rewiring probability  $p_r$ , the parameter  $\beta$  increases rapidly from  $1.02 \pm 0.053$  at  $p_r = 0$  to  $1.95 \pm 0.065$  at  $p_r = 0.14$ . For  $p_r > 0.14$ ,  $\beta$  are almost same, namely  $\sim 2.0$ . That is, the representative eigenvector changes from a nearly localized state ( $p_r = 0$ ) to an extended state in this interval of  $p_r$ . For the networks with  $p_r > 0.14$ , the representative eigenvectors are almost perfectly extended. While for the BASF networks, with the increase of  $w$ , the more edges can induce the significant extensions of the representative states.  $\beta$  reaches its asymptotic value  $\sim 1.90$ . Due to the heterogeneity, the BASF networks can not reach a perfectly extended state.

In a considerable wide range of  $q$ , the partition functions behave scale-invariant as in Eq.(8). There are three kinds of typical WT transform results. Here we present several typical examples. In the whole range of  $q = -5 \sim 5$ , the WSSW network with  $p_r = 0.05$  and the BASF network with  $w = 8$  are multi-fractal with only one characteristic point ( $h_c, D(h_c)$ ), as shown in Fig.4 and Fig.5, respectively. Sometimes, the multi-fractal degenerates to mono-fractal. Fig.6 gives another condition where the fractal behaviors can be separated into two branches, namely,  $q < 0$  and  $q > 0$ . The characteristic points for these two branches are not same. That is, the principal subsets for the large fluctuations and the small fluctuations are different. These three conditions are called mono-fractal, multi-fractal and branched multi-fractal, respectively.

The scaling properties for the real world networks and the modeling networks are listed in Table I. For the mono- and multi-fractals, we present simply the global Hurst exponent  $H$  and the characteristic point ( $h_c, D(h_c)$ ), respectively. For the branched multi-fractal we give the scaling characteristics for the two branches  $q < 0$  and  $q > 0$ , which are separated by the division symbol "/". To cite an example, for the cellular network *M.jannaschii*, the characteristic point for the branch  $q < 0$  is (0.63, 0.96) and that for the branch  $q > 0$  is (0.83, 1.03). It is denoted with (0.63, 0.96)/(0.83, 1.03). The results for the corresponding shuffled series are presented also. We discard the networks that the scaling behaviors of the original  $\rho$  and the randomized series  $\rho_R$  are undistinguishable. The sizes of the WSSW and BASF networks are  $N = 2000$ .  $N = 1000, 3000$  and  $4000$  lead almost same results (not shown in Table.1).

The WSSW and BASF networks are almost all mono-

or multi-fractals with the values of  $h_c$  mainly in the range of  $0.66 \pm 0.05$ . However, most of the considered real world networks behave branched multi-fractal. The Hurst exponents larger than 1 and near 0 correspond to non-singularity and white noises, respectively. Discarding these trivial conditions, we find that the multi-fractal behaviors are embedded in the branches of  $q > 0$ . And the values of  $h_c$  are basically in the range of  $0.8 \pm 0.05$ . The larger values of  $h_c$  for the large fluctuations in the real world networks show us the much more non-homogeneous structures of the PDF of  $\rho$ . That is, the PDF of  $\rho$  for the real world networks tend to form much sharper peaks at different scales.

It should be noted that in the present paper the structure-induced localization is used as a probe of structure properties of complex networks. We detect the localization properties for the WSSW, BASF model networks and the cellular networks, but it dose not imply and require any localization-related dynamical process (such as waves) occurring on the real-world systems.

## V. CONCLUSIONS

In summary, the probability distribution function of the representative eigenvector is proposed to describe the localization properties of complex networks. The localization quantities ( $Q, S_{str}$ ), the PDFs of the NNLS and the wavelet transform are used to capture the characteristics of the representative state. The nontrivial structures of the networks can induce the localizations of the representative states. At the same time, because of the global symmetries of the networks, the representative state have nontrivial structures rather than the step-like distribution.

The localization quantities ( $Q, S_{str}$ ) and Brody distribution parameter  $\beta$  can describe the nontrivial localization properties in a global way. The ( $Q, S_{str}$ ) values tell us that the BASF networks with  $w = 2$  are significantly localized compared with the WSSW networks with  $d = 2$ . It is consistent with the conclusions drawn from the results of  $\beta$ . The whole cellular networks have localization properties much closer with the WSSW networks.

The wavelet transform can tell us the details on the nontrivial structures of the representative eigenvectors. The ascend-ranked series  $\rho$  for the WSSW and BASF modeling networks and the whole cellular networks behave mono-fractal, multi-fractal or branched multi-fractal. The PDF of  $\rho$  tends to form sharp peaks at different scales in a self-similar way.

This kind of property can shed light on the global symmetries due to the general rules in the construction of the networks. Hence, it can be employed as a global measure of the network structures. Moreover, the structure-induced localizations on networks maybe helpful to understand the electronic conduction and heat transport properties [44] of nanonet materials.

A closely relevant topic is the diffusion on complex net-

works. Kim et al. [45] report for the first time their works on quantum and classical diffusion on WSSW networks. The Hamiltonian is same as that in the present paper, namely  $\varepsilon_n = 0$  and  $t_{mn} = 1$  in Eq.(1). An electron is localized at a randomly selected node at beginning, then the diffusion process is obtained by solving the time-dependent Schrodinger equation. It is found that the "long-range" edges can fasten the diffusion speeds significantly, especially at the transition point from  $p_r = 0$  to  $p_r \neq 0$ . This is qualitatively in consistent with our findings of the significant changes of the participation ratio and the structural entropy, ( $Q, S_{str}$ ), when  $p_r$  increase from  $p_r = 0$  to  $p_r = 0.02$ .

As for the classical diffusion on networks, a very recent work reports the first-passage times (FPT) of random walkers in complex scale-invariant media [13, 46]. Many real-world networks have self-similar structures, and diffusion on networks can be regarded to a certain degree as the diffusion on fractal media, which has attracted intensive attentions for its importance in theories and potential use in diverse research fields [47].

However, we should point out that, it is not trivial to compare our results quantitatively with these evolution processes. Actually our results are obtained from the eigenstates in energy representation, while for the quantum diffusion the initial state of localizing at a randomly selected node is a wave packet and the final state should be a superposition of the eigenstates in energy representation. How to relate the localization with the classical diffusion is definitely interesting but not a trivial task. Obviously, detailed works on diffusion on complex networks are required to understand the relation between localization and diffusion on networks.

### Acknowledgements

The work is supported by NUS Faculty Research Grant No. R-144-000-165-112/101. It is also supported by the National Science Foundation of China under Grant Nos.70571074 and 10635040. H. Yang gratefully acknowledges the support of K.C.Wong Education Foundation, Hong Kong.

- 
- [1] D. J. Watts, *Small Worlds* (Princeton University Press, Princeton, 1999); R. Albert and A. -L. Barabasi, *Rev. Mod. Phys.* **74**, 47 (2002); S. N. Dorogovtsev and J. F. F. Mendes, *Evolution of Networks* (Oxford University Press, New York, 2003).
- [2] D. J. Watts and S. H. Strogatz, *Nature* **393**,440(1998).
- [3] A. -L. Barabasi and R. Albert, *Science* **286**,509(1999).
- [4] R. Milo, S. Shen-Orr, S. Itzkovitz, N. Kashtan, D. Chklovskii, and U. Alon, *Science* **298**,824(2002).
- [5] E. Ravasz, A. L. Somera, D. A. Mongru, Z. N. Oltvai, and A.-L. Barabasi, *Science* **297**,1551(2002).
- [6] C. Song, S. Havlin, and H. A. Makse, *Nature* **433**,6392(2005); C. Song, S. Havlin, and H. A. Makse, *Nature Physics* **2**,275(2006).
- [7] L. K. Gallos, C. Song, S. Havlin, and H. A. Makse, *Proc. Natl. Acad. Sci. USA* **104**,7751(2007).
- [8] H. Yang, C. Yin, G. Zhu, and B. Li, *Phys. Rev. E* **77**,045101(R)(2008).
- [9] B. J. Kim, *Phys. Rev. Lett.* **93**,168701(2004).
- [10] M. E. J. Newman, *SIAM Review* **45**, 167(2003).
- [11] C. Zhou, and J. Kurths, *Chaos* **16**, 015104(2006); K. Park, Y. Lai, and S. Gupte, *Chaos* **16**, 015105(2006).
- [12] V. Sood, and P. Grassberger, *Phys. Rev. Lett.* **99**, 098701 (2007).
- [13] L. D. F. Costa, and G. Travieso, *Phys. Rev. E* **75**,016102(2007).
- [14] A. S. Ribeiro, S. A. Kauffman, J. Lloyd-Price, B. Samuelsson, and J. E. S. Socolar, *Phys. Rev. E* **77**,011901(2008); P. Krawitz, and I. Shmulevich, *Phys. Rev. E* **76**,036115(2007).
- [15] K.-I. Goh, B. Kahng, and D. Kim, *Phys. Rev. E* **64**,051903 (2001); S. N. Dorogovtsev, A. V. Goltsev, J. F. Mendes, and A. N. Samukhin, *Phys. Rev. E* **68**,046109 (2003); C. Zhu, S. Xiong, Y. Tian, N. Li and K. Jiang, *Phys. Rev. Lett.* **92**, 218702 (2004); C. Kamp, and K. Christensen, *Phys. Rev. E* **71**,041911(2005); M. Sade, T. Kalisky, S. Havlin, and R. Berkovits *Phys. Rev. E* **72**,066123(2005); P. N. McGraw, and M. Menzinger, *Phys. Rev. E* **75**,027104(2007); J. N. Bandyopadhyay and S. Jalan, *Phys. Rev. E* **76**,026109(2007).
- [16] H. Yang, F. Zhao, L. Qi, and B. Hu, *Phys. Rev. E* **69**,066104(2004); F. Zhao, H. Yang, and B. Wang, *Phys. Rev. E* **72**,046119(2005); H. Yang, F. Zhao, and B. Wang, *Physica A* **364**,544(2006); H. Yang, F. Zhao, and B. Wang, *Chaos* **16**,043112(2006).
- [17] S. Xiong and S.N. Evangelou, *Phys. Rev. B* **52**,13079(R)(1995); C. Zhu, and S. Xiong, *Phys. Rev. B* **62**,14780(2000); L. Gong, and P. Tong, *Phys. Rev. E* **74**,056103(2006).
- [18] J. Yi, B. J. Kim, *Phys. Rev. B*, **76**,245207(2007).
- [19] M. Dresselhaus, G. Dresselhaus, P. Eklund, and R. Saito, *Phys. World* **11**,33(1998); P. G. Collins, and P. Avouris, *Sci. Am.* **283**,62(2000); R. H. Baughman, A. A. Zakhidov, and W. A. de Heer, *Science* **297**,787(2002); G. Gruner, *J. Mat. Chem.* **16**,3533(2006); G. Gruner, *Anal. Bio. Chem.* **384**,322(2006); G. Gruner, *Sci. Am.* **17**,48(2007).
- [20] E. Lopez, S. V. Buldyrev, S. Havlin, and H. E. Stanley, *Phys. Rev. Lett.* **94**,248701(2005); Z. Wu, L. A. Braunstein, S. Havlin, and H. E. Stanley, *Phys. Rev. Lett.* **96**,148702(2006); G. Li, L. A. Braunstein, S. V. Buldyrev, S. Havlin, and H. E. Stanley, *Phys. Rev. E* **75**,R045103(2007).
- [21] P. W. Anderson, *Phys. Rev.* **109**, 1492(1958); P. A. Lee, and T. V. Ramakrishnan, *Rev. Mod. Phys.* **57**,287(1985).
- [22] Y.-J. Kim, M. H. Lee, and M. Y. Choi, *Phys. Rev. B* **40**, 2581(1989).
- [23] M. Titov, and H. Schomerus, *Phys. Rev. Lett.* **91**, 176601(2003).
- [24] C. Tang, and M. Kohmoto, *Phys. Rev. B* **34**, 2041(1986).
- [25] M. Kohmoto, B. Sutherland, and C. Tang, *Phys. Rev. B* **35**, 1020(1987).
- [26] M. Mezard, G. Parisi, and A. Zee, *Nucl. Phys. B* **559**, 689(1999); S. Ciliberti, T. S. Grigera, V. Martn-



- Mayor, G. Parisi, and P. Verrocchio, *Phys. Rev. B* **71**, 153104(2005).
- [27] M. Sade, and R. Berkovits, *Phys. Rev. B* **68**,193102(2003).
- [28] E. L. Albuquerque and M. G. Cottam, *Phys. Rep.* **376**,225(2003).
- [29] M. Janssen, *Phys. Rep.* **295**, 1 (1998).
- [30] A.D. Mirlin, *Phys. Rep.* **326**, 259 (2000).
- [31] J. Pipek and I. Varga, *Phys. Rev. A* **46**,3148 (1992).
- [32] J. Pipek, *Phys. Rev. E* **68**,026202 (2003); and the references there-in.
- [33] I. Varga, *Phys. Rev. B* **66**,094201 (2002).
- [34] T. Guhr, A. Muller-Groeling, and H. A. Weidenmuller, *Phys. Rep.* **299**, 189(1998).
- [35] T. Dittrich, *Phys. Rep.* **271**,267(1996).
- [36] R. Berkovits and Y. Avishai, *Phys. Rev. B* **53**, R16125(1996).
- [37] B. L. Altshuler, I. Kh. Zharekeshev, S. A. Kotochigova, and B. I. Shklovskii, *Zh. Eksp. Teor. Fiz* **94**, 343(1988) [*Sov. Phys. JETP* **67**,625(1988)].
- [38] B. I. Shklovskii, B. Shapiro, B. R. Scars, P. Lambrianides, and H. B. Shore, *Phys. Rev. B* **47**, 11487(1993).
- [39] E. Hofstetter and M. Schreiber, *Phys. Rev. B* **48**,16979(1993).
- [40] M.L. Goldstein, S.A. Morris, and G.G. Yen, *Eur.Phys. J. B* **41**,255(2004); M. E. J. Newman, *Contemp. Phys.* **46**,323(2005); A. Clauset, C. R. Shalizi, and M. E. J. Newman, arXiv:0706.1062v1.
- [41] P. CH. Ivanov, L. A. N. Amaral, A. L. Goldberger, S. Havlin, M. G. Rosenblum, Z. R. Struzik, and H. E. Stanley, *Nature* **399**,461(1999).
- [42] H. Jeong, B. Tombor, R. Albert, Z. N. Oltvai, and A.-L. Barabasi, *Nature* **407**,651(2000).
- [43] R. Overbeek, et al., *Nucleic Acid Res.* **28**,123(2000). see also, <http://igweb.integratedgenomics.com/IGwit>.
- [44] Z. Liu, and B. Li, *Phys. Rev. E* **76**,051118(2007).
- [45] B. J. Kim, H. Hong, and M. Y. Choi, *Phys. Rev. B* **68**,014304(2003).
- [46] S. Condamin, O. Benichou, V. Tejedor, R. Voituriez, and J. Klafter, *Nature* **450**,77(2007).
- [47] F. D. A. Aarao Reis, *J. Phys. A* **29**7803(1996); C. Schulzky, A. Franz, and K. H. Hoffmann, *SIGSAM Bull.* **34**,1(2000); A. Franz, C. Schulzky, S. Tarafdar, and K. H. Hoffmann, *J. Phys. A* **34**,8751(2001); D. H. N. Anh, K. H. Hoffmann, S. Seeger, and S. Tarafdar, *Europhys. Lett.* **70**,109(2005); D. H. N. Anh, P. Blaudeck, K. H. Hoffmann, J. Prehl and S. Tarafdar, *J. Phys. A* **40**,11453(2007).